



Wind composition beyond the tip of the AGB and its relevance to stardust grains

J. Buntain¹, M. Lugaro¹, R. J. Stancliffe¹, A. Karakas², L. Nittler³, and P. Hoppe⁴

¹ Centre for Stellar and Planetary Astrophysics, Monash University, Clayton, Victoria 3800, Australia, e-mail: Joeline.Buntain@sci.monash.edu.au

² Research school of Astronomy & Astrophysics, Mount Stromlo Observatory, Weston Creek, Canberra, ACT 2611, Australia

³ Department of Terrestrial Magnetism, Carnegie Institution of Washington, 5241 Broad Branch Road NW, Washington, DC 20015, USA

⁴ Max-Planck-Institute for Chemistry, Particle Chemistry Department, J.-J.-Becherweg 27, D-55128, Mainz, Germany

Abstract. After its H-rich envelope is reduced to a small mass, less than around 10^{-2} – $10^{-3} M_{\odot}$, an asymptotic giant branch (AGB) star evolves to become a post-AGB star and then may become the central star of a planetary nebula. In these phases, the star evolves at a constant luminosity to hotter temperatures while the mass of the thin H-rich region decreases because of winds. We investigate the isotopic composition of this wind, which shows the signature of H burning. We compare our predictions to the composition measured in Group II stardust oxide and silicate grains to assess the hypothesis that some of this dust formed from material ejected by post-AGB stars and planetary nebula nuclei. We find that the composition of this H-rich region is very close to that of Group II grains, especially if some mixing of the different layers within the region is performed. The problem is that the total mass involved appears to be too small to reproduce the frequency of Group II grains. However, we cannot exclude this origin for Group II grains because their frequency would also be determined by the uncertain mechanism of grain formation in post-shock regions produced when fast winds from a planetary nebula central star collide with the material surrounding the star.

Key words. Stars: AGB and Post-AGB – Grains: Presolar – Grains: Population II – Isotopes – Post-AGB-winds – Meteorites

1. Introduction

After very dense and slow winds erode the outer layer of an asymptotic giant branch (AGB) star down to a thin H-rich layer of less than about $10^{-2} M_{\odot}$, the star becomes a post-AGB star and evolves at constant luminosity towards hotter temperatures (van Winckel,

2003). Material around the star expelled by the earlier AGB wind can be illuminated by the photons coming from the central star before dissipating into the interstellar medium. A planetary nebula is formed and the central star becomes known as a planetary nebula nucleus (PNN). During these phases, the thin H-rich

surface layer of the star is eroded by winds. In particular, very fast winds occur from PNN. These winds are much less dense than the typical AGB winds because the mass loss rate is of the order of $10^{-7} - 10^{-8} M_{\odot} \text{yr}^{-1}$ compared with up to $10^{-4} - 10^{-5} M_{\odot} \text{yr}^{-1}$ during the AGB phase. On the other hand they are much faster as they can reach a speed of the order of 10^3 km s^{-1} , while the speed of AGB wind is around 30 km s^{-1} . These PNN winds cause dramatic effects by dynamically interacting with the material that exists around the central stars from the previous AGB wind episodes (see, e.g., Grewing, 1989). Eventually, the central star cools to become a CO white dwarf, with a typical H-rich layer of about $10^{-4} M_{\odot}$ or less (see MacDonald & Vennes, 1991).

The aim of this paper is to analyse the composition of post-AGB and PNN winds and compare them to the composition of meteoritic stardust grains. These are tiny and rare dust grains with a stellar origin that predates the formation of the solar system. They did not homogenize with the bulk of the material that formed our Sun but survived the solar system formation as individual microcrystals and were trapped in primitive meteorites. Today they are recovered from meteorites and analysed in the laboratory as solid samples of stars (see review by Clayton & Nittler, 2004). Stardust grains are recognised for their highly unusual isotopic ratios, which display enormous anomalies of up to four orders of magnitude with respect to the solar system composition. Some grains initially formed in gas surrounding the envelope of the giant stars. Some others are believed to have formed in the ejecta from nova and supernova explosions. The vast majority of them originated from AGB stars.

From stardust, various oxide and silicate grains, including corundum (Al_2O_3), spinel ($\text{Mg Al}_2\text{O}_4$) and Si O_2 , all of which form in O-rich ($\text{O} > \text{C}$) gas, have been recovered. The vast majority of these Group I grains show the signature of an origin in red giant or AGB stars. This is because their oxygen isotopic ratios – ^{17}O excesses with respect to solar – are compatible with those observed and predicted in stars after the first dredge-up has occurred when the star reaches the red giant branch for

the first time. However, some 10–15% of oxide and silicate grains (Group II) show significant depletions in ^{18}O , from $^{18}\text{O}/^{16}\text{O} \approx 0.001$ down to very anomalous values as low as 10^{-5} , two orders of magnitude below solar. The initial presence of the radioactive nucleus ^{26}Al has also been inferred from excesses in its daughter nucleus ^{26}Mg , with $^{26}\text{Al}/^{27}\text{Al}$ ratios up to 0.1 (Nittler et al., 1997).

The origin of Group II grains is still unclear. The current explanation of their composition is some kind of extra-mixing process in AGB stars. Such mixing would circulate material from the convective envelope to below its base into the deeper radiative layers where H burning is active. This process can explain the grain compositions, depending on the depth and the rate of the mixing (Nollett et al., 2003). However, the physical mechanism responsible for such deep mixing remains unclear (even though work is in progress on this problem, Busso et al., 2007; Denissenkov et al., 2009) and it is debated whether this mechanism is really needed to explain stellar observations (Karakas et al., 2010). Another problem with this scenario is that only a few AGB stars overlap the region occupied by Group II grains in the $^{16}\text{O}/^{17}\text{O}$ against $^{16}\text{O}/^{18}\text{O}$ plot, and these are C-rich stars, while oxide grains can only form if $\text{C} < \text{O}$ (see fig. 9 of Nittler et al., 1997). So, the AGB parent stars of the more extreme grains have not been officially identified, although this may be due to observational selection effects.

In this paper we wish to test an alternative explanation for the composition of oxide and silicate stardust grains of Group II by linking their origin to the wind episodes that occur beyond the tip of the AGB and carry the signature of the H-burning material that gets progressively exposed at the stellar surface.

2. Methods and results

To look at the composition of post-AGB and PNN winds we took a $1.25 M_{\odot}$ model of solar metallicity from Karakas & Lattanzio (2007) and selected the deepest $10^{-3} M_{\odot}$ H-rich region of the star during a typical interpulse period. A snapshot of the composition profile in this re-

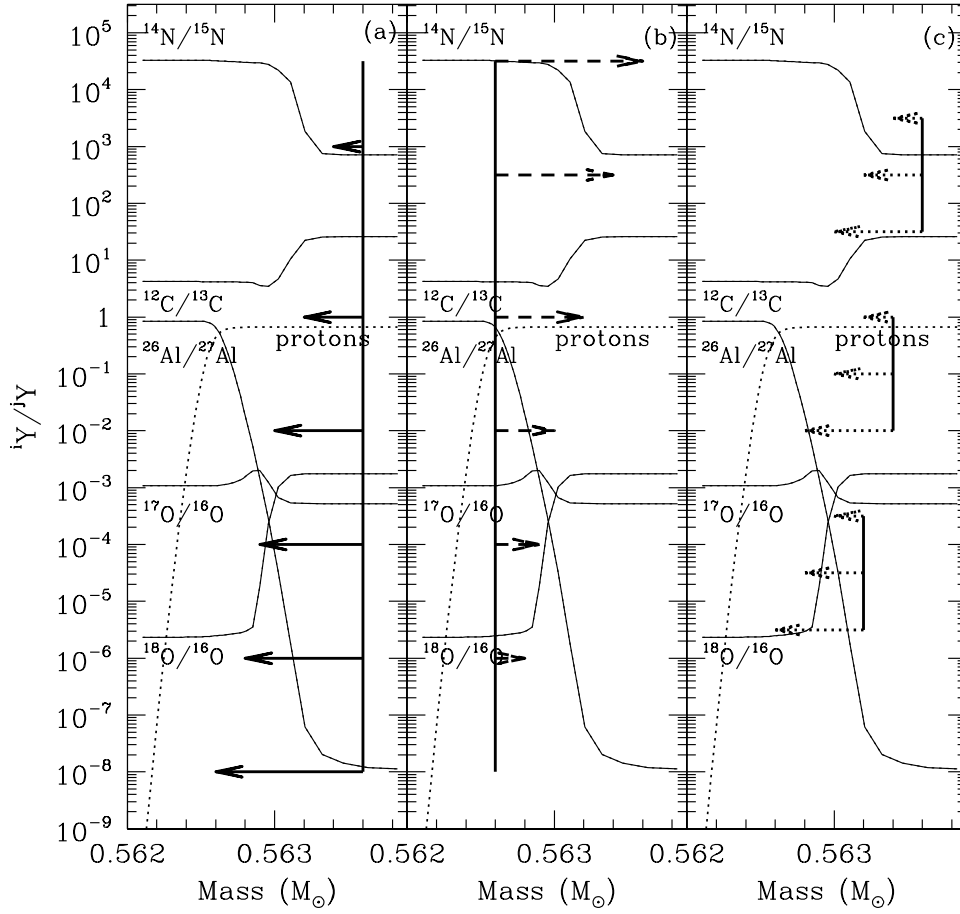


Fig. 1. Each panel shows the same isotopic ratios as a function of the position in mass in the deepest $10^{-3} M_{\odot}$ H-rich layer (in between $0.5626 M_{\odot}$ and $0.5636 M_{\odot}$) during a typical interpulse period for a $1.25 M_{\odot}$ AGB star of $Z = 0.02$. We assume this material is representative of the material lost in the winds after the tip of the AGB. The dotted black line represents the abundance of protons and helps locate the underlying H-burning shell at roughly $0.5625 M_{\odot}$. This composition clearly shows the signature typical of H-burning. The arrows schematically illustrate how the theoretical lines labelled “mixed” in Figs 2 and 3 were obtained starting from the plotted composition. The mixing was performed by taking the mass-weighted integral of each isotopic abundance over a range of mesh points. The arrows in (a) indicate that the mixing was performed over the whole mass region starting from the outer and moving toward the inner layers. Each open diamond connected by a solid line in Figs 2 and 3 is obtained by adding one more mesh point to the average. The arrows in (b) indicate that the mixing was performed over the whole mass region starting from the inner and moving toward the outer layers. Each open circle connected by a long-dashed line in Figs. 2 and 3 is obtained by adding one more mesh point to the average. The arrows in (c) indicate that the mixing was performed over different mass sub-regions within the given range, starting from the outer point and moving towards the inner point of each sub-region. For sake of clarity only three mass sub-regions are schematically indicated in this panel. In reality we selected six mass sub-regions resulting in six short-dashed lines in Figs 2 and 3. Each open square on these lines is again obtained by adding one more mesh point to the average.

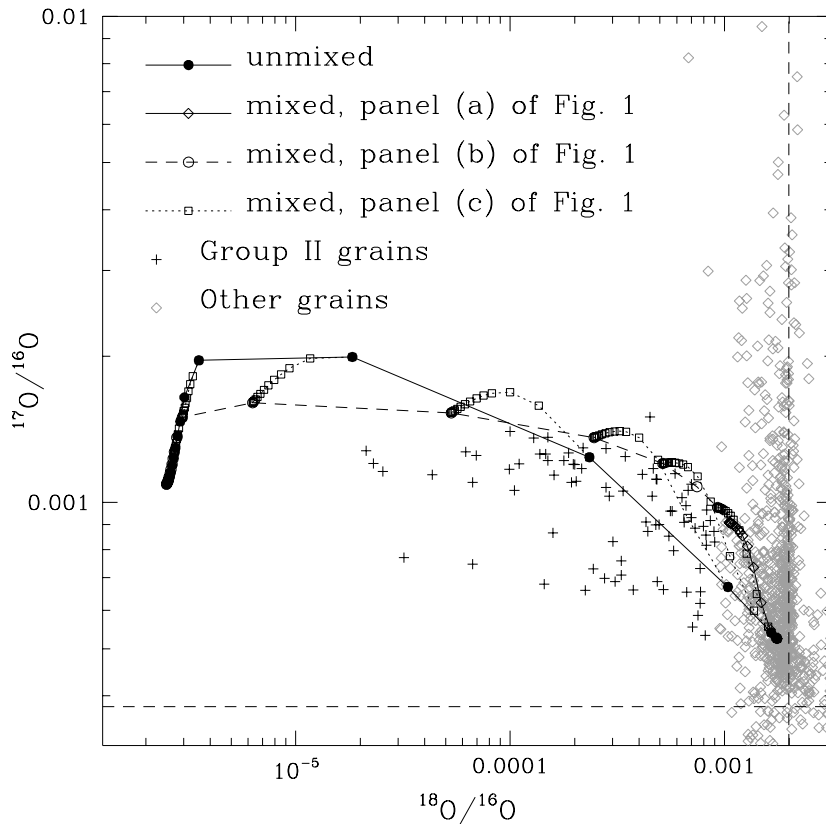


Fig. 2. The $^{17}\text{O}/^{16}\text{O}$ against $^{18}\text{O}/^{16}\text{O}$ isotopic ratios corresponding to the stratified composition (unmixed, solid line with black circles) and to the mixed composition from the different mixing schemes illustrated by the arrows in Fig. 1 are compared to data for oxide and silicate stardust grains. Vertical and horizontal dashed lines represent the solar values.

gion is shown in Fig. 1. We simulated the mixing of this material as it may occur in the winds or during the interaction of the winds with the surrounding material. We experimented with different types of mixing possibilities, which are illustrated in Fig. 1. In Figs. 2 and 3 we present the O and Al compositions obtained by keeping the material stratified (unmixed) or mixed in the different ways described in Fig. 1 and compare them to the stardust data points.

Looking closely at the comparison with the data presented in Figs. 3 and 4 we notice that the unmixed compositions do not provide a very close match to the Group II grains.

Mixing from the outer to the inner layers of the star (solid line with diamonds on top) as shown by the arrows in panel (a) of Fig. 1 did not allow us to move far enough from solar composition to reach Group II grains. Mixing from the inner to the outer layer of the star (long-dashed line with open circles on top) as shown by the arrows in panel (b) of Fig. 1 provided a somewhat better match to the data. When mass subregions over which to mix were selected and the mixing was performed from the outer to the inner layers of the star (short-dashed lines with open squares on top) as shown by the arrows in panel (c) of Fig. 1, we can cover the majority of

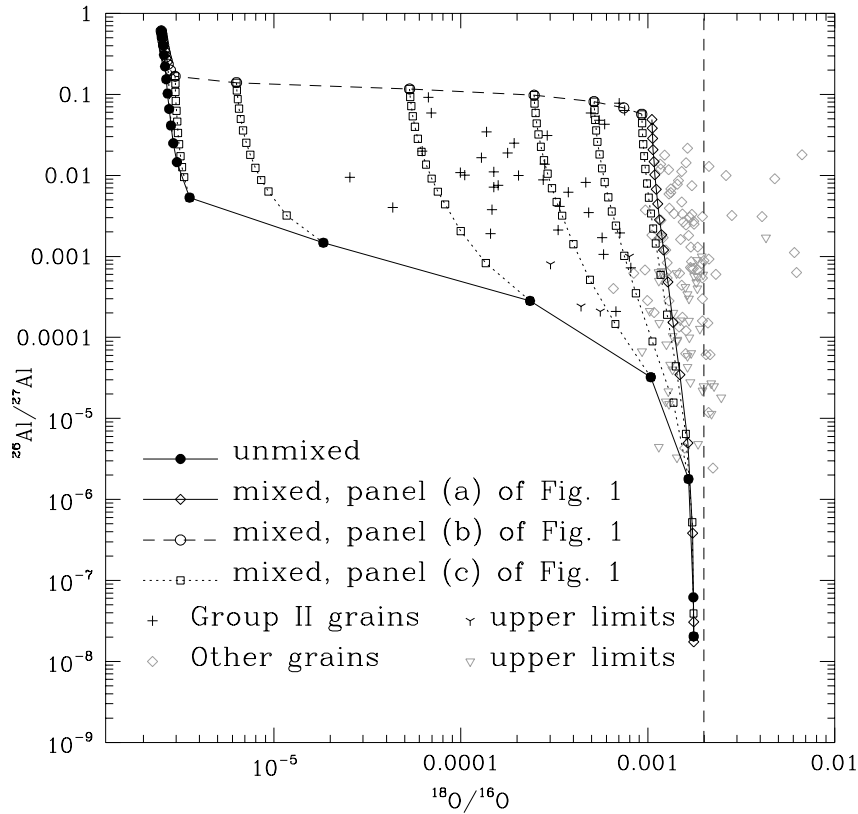


Fig. 3. Same as Fig. 2 but for the $^{26}\text{Al}/^{27}\text{Al}$ against $^{18}\text{O}/^{16}\text{O}$ isotopic ratios.

the $^{26}\text{Al}/^{27}\text{Al}$ grain data, while the $^{17}\text{O}/^{16}\text{O}$ remains roughly 50% higher than the data points.

3. Discussion

A main result of our tests is that to match the Group II grains we need to mix within the inner half of the total $10^{-3} M_{\odot}$ mass we are considering. In fact, if we include in the mixture too much material from the outer half of the mass range, we quickly move towards $^{18}\text{O}/^{16}\text{O}$ ratios greater than 0.001. The main problem of this scenario is that the total mass involved in the grain formation process must be very small. Since the mass of the AGB envelope lost during AGB winds, where the vast majority of oxide and silicate grains form, is about $0.7 M_{\odot}$,

the mass considered here represents less than 0.1% of the total mass lost in the stellar winds. On the other hand, approximately 10 – 15% of presolar oxides and silicate grains belong to Group II.

However, there may be selection effects related to the grain size distribution and affecting the number of grains. First, the stardust grains analysed in the laboratory have sizes larger than about $0.3 \mu\text{m}$ (see, e.g., Fig. 4 of Nittler et al., 1997) while the vast majority of the grains ejected by oxygen-rich mass-losing red giants are smaller than $0.3 \mu\text{m}$ (Jura, 1996). Secondly, in the scenario proposed here Group II grains may have formed in the post-shock regions resulting when PNN fast winds col-

lide with the surrounding material. These regions are observed as X-ray emitting regions (e.g. Akashi et al., 2006). This would indicate a temperature too high for dust formation. However, dust is observed to form in post-shock regions in different environments, from the colliding winds of binary massive stars like Eta Carinae and Wolf Rayet stars of WC type, to supernovae post-shock regions (see Smith, 2010, and references therein). We do not know enough about the efficiency of grain formation in post-shock regions in planetary nebulae, and the resulting grain size distribution and features, to make a definite conclusion on the viability of our scenario. In relation to the formation of dust we need to point out that formation of oxide grains is allowed in the material we have considered here because it has a $C/O < 1$. This is because we have considered a stellar model that does not experience any dredge-up of material from the He- and C-rich region into the envelope during its AGB phase. This is typically verified, at solar metallicities, for stellar masses less than about $1.5 - 2 M_{\odot}$, depending on the stellar code. Higher stellar masses would instead more likely have $C/O > 1$ in the material expelled in their PNN winds. This composition should also be investigated in detail because it may be relevant to the composition of stardust silicon carbide (SiC) grains belonging to the A+B population, the origin of which is still unknown (Amari et al., 2001). Some of these grains shown the signature of H-burning in their composition, with low $^{13}C/^{12}C$ and high $^{14}N/^{15}N$ and $^{26}Al/^{27}Al$ ratios, and they can form only if $C/O > 1$.

Future work will analyse the composition profiles for different interpulse periods and stellar masses. We also need to check the compositions that result when some material from the deeper He-rich region of the star is added to the mixture. This may happen because mixing episodes are related to late thermal pulses during the post-AGB phase (Blöcker, 2001). He-rich material is observed in these regions in the X-ray (Murashima et al., 2006; Yu et al., 2009). It is also testified by the composition of the noble gases He and Ne in meteoritic silicon carbide grains from AGB stars, where the noble

gases were implanted in the stardust after being ionised in the fast PNN winds (Verchovsky et al., 2004). The He-rich material contains ^{16}O but insignificant amounts of ^{17}O and ^{18}O , because these are destroyed by He burning, so it may shift the predicted O composition closer to that of the grains. It may also contain a peculiar Mg composition, with excesses in the heavy Mg isotopes produced by $^{22}Ne + \alpha$ reactions. These we also need to analyse in detail and compare to data on Mg isotopic ratios from stardust spinel grains.

References

- Akashi, M., Soker, N., & Behar, E. 2006, *MNRAS*, 368, 1706
- Amari, S., Nittler, L. R., Zinner, E., Lodders, K., & Lewis, R. S. 2001, *ApJ*, 559, 463
- Blöcker, T. 2001, *Ap&SS*, 275, 1
- Busso, M., Wasserburg, G. J., Nollett, K. M., & Calandra, A. 2007, *ApJ*, 671, 802
- Clayton, D. D. & Nittler, L. R. 2004, *ARA&A*, 42, 39
- Denissenkov, P. A., Pinsonneault, M., & MacGregor, K. B. 2009, *ApJ*, 696, 1823
- Grewing, M. 1989, in *IAU Symposium 131, Planetary Nebulae*, ed. S. Torres-Peimbert (Reidel, Dordrecht), 241
- Jura, M. 1996, *ApJ*, 472, 806
- Karakas, A. & Lattanzio, J. C. 2007, *PASA*, 24, 103
- Karakas, A. I., Campbell, S. W., & Stancliffe, R. J. 2010, *ApJ*, 713, 374
- MacDonald, J. & Vennes, S. 1991, *ApJ*, 371, 719
- Murashima, M., Kokubun, M., Makishima, K., et al. 2006, *ApJ*, 647, L131
- Nittler, L. R., Alexander, C. M. O., Gao, X., Walker, R. M., & Zinner, E. 1997, *ApJ*, 483, 475
- Nollett, K. M., Busso, M., & Wasserburg, G. J. 2003, *ApJ*, 582, 1036
- Smith, N. 2010, *MNRAS*, 402, 145
- van Winckel, H. 2003, *ARA&A*, 41, 391
- Verchovsky, A. B., Wright, I. P., & Pillinger, C. T. 2004, *ApJ*, 607, 611
- Yu, Y. S., Nordon, R., Kastner, J. H., et al. 2009, *ApJ*, 690, 440